Eur Phys J A (2005) **24,** s1, 59–63
DOI: 10.1140/epjad/s2005-05-010-2

EPJ A direct
electronic only

Two-photon exchange in elastic electron–proton scattering

P.G. Blunden[1], W. Melnitchouk[2], and J.A. Tjon[2,3]

[1] Department of Physics and Astronomy, University of Manitoba, Winnipeg, MB, Canada R3T 2N2
[2] Jefferson Lab, 12000 Jefferson Ave., Newport News, VA 23606, USA
[3] Department of Physics, University of Maryland, College Park, MD 20742-4111, USA

Received: 27 September 2004 / Published Online: 8 February 2005

Abstract. Two-photon exchange contributions to unpolarized and polarized elastic electron–proton scattering cross sections are evaluated taking into account nucleon finite size effects using realistic form factors. Contributions from nucleon elastic intermediate states are found to have a strong angular dependence, which partially resolves the discrepancy between Rosenbluth and polarization transfer measurements of the proton electric to magnetic form factor ratio. Two-photon contributions to the longitudinal and transverse polarizations are generally found to be small. A comparison is made of two-photon exchange effects with existing data on the ratio of e^+p to e^-p cross sections, which is predicted to be enhanced at backward angles.

PACS. 25.30.Bf Elastic electron scattering – 13.40.Gp Electromagnetic form factors

1 Introduction

Electromagnetic form factors are fundamental observables which characterize the composite nature of the nucleon. In the standard one-photon exchange (Born) approximation, the electromagnetic current operator is parameterized in terms of two form factors, usually taken to be the Dirac (F_1) and Pauli (F_2) form factors,

$$\Gamma^\mu = F_1(q^2)\,\gamma^\mu + \frac{i\sigma^{\mu\nu}q_\nu}{2M}F_2(q^2)\ , \tag{1}$$

where q is the momentum transfer to the nucleon, and M is the nucleon mass. The resulting cross section depends on two kinematic variables, conventionally taken to be $Q^2 \equiv -q^2$ (or $\tau \equiv Q^2/4M^2$) and either the scattering angle θ, or the virtual photon polarization $\varepsilon = \left(1+2(1+\tau)\tan^2(\theta/2)\right)^{-1}$. In terms of the Sachs electric and magnetic form factors, defined as

$$G_E(Q^2) = F_1(Q^2) - \tau F_2(Q^2)\ , \tag{2}$$
$$G_M(Q^2) = F_1(Q^2) + F_2(Q^2)\ , \tag{3}$$

the reduced Born cross section can be written

$$\sigma_R = G_M^2(Q^2) + \frac{\varepsilon}{\tau}G_E^2(Q^2)\ . \tag{4}$$

The Rosenbluth, or longitudinal-transverse (LT), separation method extracts G_M^2 from the ε-intercept, and the ratio $R \equiv \mu G_E/G_M$ from the slope in ε, where μ is the nucleon magnetic moment. The results of the Rosenbluth measurements for the proton have generally been consistent with $R \approx 1$ for $Q^2 \leq 6$ GeV^2 [1,2]. The "Super-Rosenbluth" experiment at Jefferson Lab [3], in which smaller systematic errors were achieved by detecting the recoiling proton rather than the electron, as in previous measurements, is also consistent with the earlier LT results.

Alternatively, the ratio R was measured recently at Jefferson Lab [4] by using a polarized electron beam scattering from an unpolarized target, with measurement of the polarization of the recoiling proton. From the ratio of the transverse to longitudinal recoil polarizations one finds

$$R = -\mu\frac{P_T}{P_L}\frac{(E_i+E_f)}{2M}\tan\frac{\theta}{2}\ , \tag{5}$$

where E_i and E_f are the initial and final electron energies, and P_T (P_L) is the polarization of the recoil proton transverse (longitudinal) to the proton momentum in the scattering plane.

The polarization transfer experiments yield strikingly different results compared with the LT separation, with $R \approx 1 - 0.135(Q^2/\text{GeV}^2 - 0.24)$ over the same range in Q^2 [2].

In this contribution we will discuss calculations of radiative corrections, in particular two-photon exchange, and how it affects both measurements.

2 Unpolarized electron–proton scattering

Including radiative corrections (RC) to order α, the elastic scattering cross section is modified as

$$\sigma_R \to \sigma_R(1+\delta)\ , \tag{6}$$

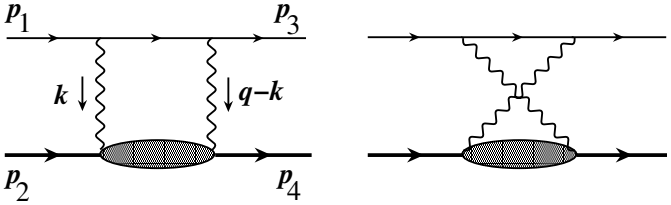

Fig. 1. Two-photon exchange box and crossed box diagrams for elastic electron–proton scattering

where δ includes one-loop virtual corrections of order α (vacuum polarization, electron and proton vertex, and two photon exchange corrections), as well as the inelastic brem-sstrahlung for real photon emission [5].

For the LT separation technique, one extracts the ratio R^2 from the ε dependence of the cross section at fixed Q^2. Because of the factor ε/τ multiplying G_E^2 in (4), the cross section becomes dominated by G_M with increasing Q^2, while the relative contribution of the G_E term is suppressed. Hence understanding the ε dependence of the radiative correction δ becomes increasingly important at high Q^2. As pointed out in [2], for example, a few percent change in the ε slope in $d\sigma$ can lead to a sizable effect on R. In contrast, as we discuss later, the polarization transfer technique does not show the same sensitivity to the ε dependence of δ.

In general, δ is of order 25%. Fortunately, the dominant radiative corrections appearing in δ either do not depend on ε (vacuum polarization, electron vertex), or are well understood (inelastic bremsstrahlung, which enters differently depending on whether the electron or proton are detected). That leaves two-photon exchange as the only viable ε-dependent radiative correction that can account for the difference between the LT and polarization transfer measurements.

In principle the two-photon exchange amplitude $\mathcal{M}^{\gamma\gamma}$ includes all possible hadronic intermediate states in Fig. 1. Here we consider only the elastic contribution to the full response function, and assume that the proton propagates as a Dirac particle (calculations of excited state contributions are in progress [6]). We also assume that the off-shell current operator is given by (1), and use phenomenological form factors at the $\gamma^* NN$ vertices. This is, of course, the source of the model dependence in the problem. Clearly this also creates a tautology, as the radiative corrections are also used to determine the experimental form factors. However, because δ for two-photon exchange is the ratio

$$\delta = \frac{2\mathrm{Re}\left\{\mathcal{M}_0^\dagger \mathcal{M}^{\gamma\gamma}\right\}}{|\mathcal{M}_0|^2} \ , \tag{7}$$

where $\mathcal{M}_0$ is the Born amplitude, the model dependence cancels somewhat, provided we use the same phenomenological form factors for both $\mathcal{M}_0$ and $\mathcal{M}^{\gamma\gamma}$.

The dominant contribution to the box and crossed box diagrams comes from the poles at $k = 0$ and $k = q$, which lead to an infrared (IR) divergence. Typically an infinitesimal photon mass λ is introduced in the photon propagator to regulate the IR divergences. The IR divergent part is of interest since it is the one usually included in the standard RC analyses. It is also independent of hadronic structure.

The IR divergent part of the amplitude $\mathcal{M}^{\gamma\gamma}$ gives an IR divergent two-photon exchange contribution to the cross section of the form

$$\delta_{\rm IR} = -\frac{2\alpha}{\pi} \ln\left(\frac{E_i}{E_f}\right) \ln\left(\frac{Q^2}{\lambda^2}\right) \ , \tag{8}$$

a result given by Maximon and Tjon [7]. The logarithmic IR singularity in λ is exactly cancelled by a corresponding term in the bremsstrahlung cross section involving the interference between real photon emission from the electron and from the nucleon.

We are interested in the finite part of $\mathcal{M}^{\gamma\gamma}$ that is not included in the standard RC analyses. One approach is to evaluate δ using (7) with the full expression for $\mathcal{M}^{\gamma\gamma}$, and subtract the IR-divergent result (8). This gives results independent of the photon mass λ.

To compare with experimental analyses, we actually use an expression for $\delta_{\rm IR}$ from the standard treatment of Mo and Tsai (MT) [5], which we call $\delta_{\rm IR}$(MT) to distinguish it from (8). The difference $\delta_{\rm IR} - \delta_{\rm IR}$(MT) already gives a correction to the cross section of order 1% over the full range of ε [7,8].

In [8] we used a simple monopole form factor to parametrize the nucleon form factors in the loop integration for $\mathcal{M}^{\gamma\gamma}$. In the present analysis we use more realistic form factors in the loop integration, fitted to $G_{E,M}$ data. These are parametrized as a sum of 3 monopole form factors over a range in Q^2 up to ≈ 10 GeV^2. With this choice, the loop integrals can be evaluated analytically in terms of Passarino-Veltman functions [9]. In practice, we note that our numerical results have only a weak dependence on G_E, and depend principally on the experimentally better measured form factor G_M.

2.1 Proton 2γ results

To compare the ε dependence of the full calculation with that of $\delta_{\rm IR}$(MT), we consider the difference

$$\Delta \equiv \delta_{\rm full} - \delta_{\rm IR}({\rm MT}) \ , \tag{9}$$

in which the IR divergences cancel, and which is independent of λ.

The results for the difference Δ between the full calculation and the MT approximation are shown in Fig. 2 for $Q^2 = 3$ and 6 GeV^2. The additional corrections are significant at low ε, and essentially vanish at large ε. Significant deviations from linearity are observed with increasing Q^2, especially at smaller ε.

To estimate the influence of these corrections on the electric to magnetic proton form factor ratio, the simplest approach is to examine how the ε slope changes with the inclusion of the 2γ exchange. Of course, such a simplified analysis can only be approximate since the ε dependence is only linear over limited regions of ε, with clear deviations from linearity at low ε and high Q^2. In the actual data analyses one should apply the correction Δ directly to the

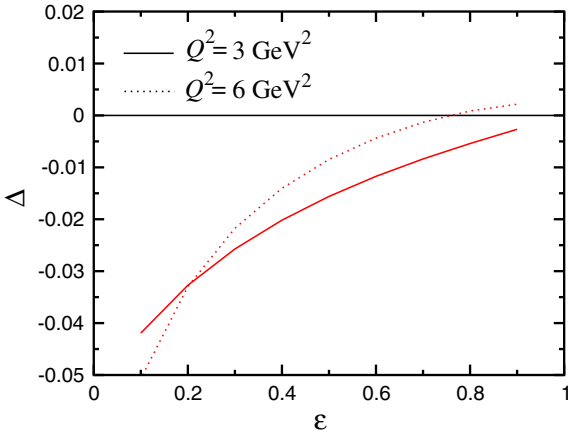

Fig. 2. Difference between the full two-photon exchange correction to the elastic cross section (using realistic form factors) and the commonly used Mo & Tsai result [5] for $Q^2 = 3$ and 6 GeV^2

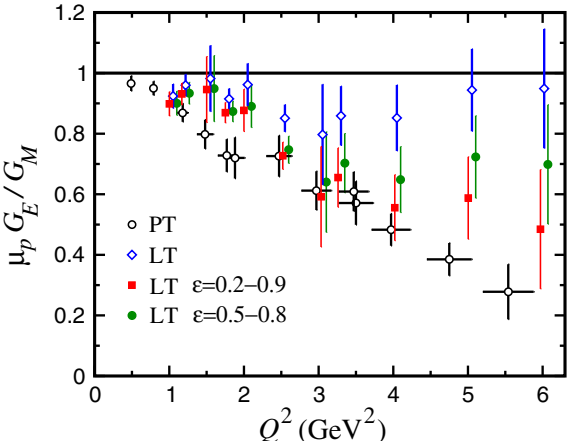

Fig. 3. The ratio of proton form factors $\mu_p G_E^p / G_M^p$ measured using LT separation (*open diamonds*) [2] and polarization transfer (PT) (*open circles*) [4]. The LT points corrected for 2γ exchange are shown assuming a linear slope for $\varepsilon = 0.2 - 0.9$ (*filled squares*) and $\varepsilon = 0.5 - 0.8$ (*filled circles*) (offset for clarity)

data. However, it is still instructive to obtain an estimate of the effect of R by taking the slope over several ranges of ε.

Following [8], this can be done by fitting the correction $(1 + \Delta)$ to a linear function of ε, of the form $a(1 + b\varepsilon)$, for each value of Q^2 at which the ratio R is measured.

The shift in R is shown in Fig. 3, together with the polarization transfer data. We consider two ranges for ε: a large range $\varepsilon = 0.2 - 0.9$, and a restricted range $\varepsilon = 0.5 - 0.8$. The approximation of linear ε dependence should be better for the latter, even though in practice experiments typically sample values of ε near its lower and upper bounds. A proposed experiment at Jefferson Lab [10] aims to test the linearity of the ε plot through a precision measurement of the unpolarized elastic cross section.

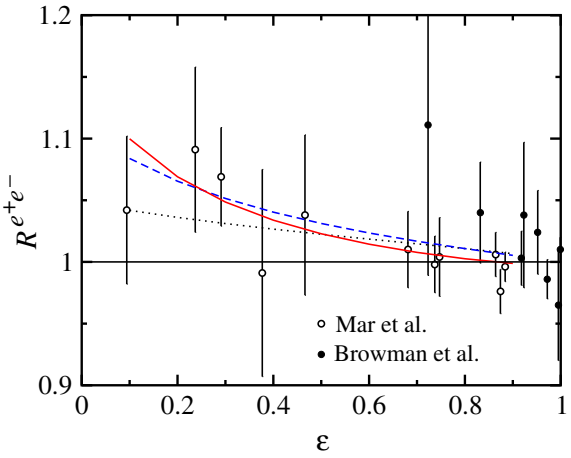

Fig. 4. Ratio of elastic e^+p to e^-p cross sections. The data are from SLAC [11,12], with Q^2 ranging from 0.01 to 5 GeV^2. The results of the 2γ exchange calculations are shown by the curves for $Q^2 = 1$ (*dotted*), 3 (*dashed*) and 6 GeV^2 (*solid*)

The effect of the 2γ exchange terms on R is clearly significant. As observed in [8], the 2γ corrections have the proper sign and magnitude to resolve a large part of the discrepancy between the two experimental techniques. In particular, the earlier results [8] using simple monopole form factors found a shift similar to that in for the $\varepsilon = 0.5 - 0.8$ range in Fig. 3, which resolves around 1/2 of the discrepancy. The non-linearity at small ε makes the effective slope somewhat larger if the ε range is taken between 0.2 and 0.9. The magnitude of the effect in this case is sufficient to bring the LT and polarization transfer points almost to agreement, as indicated in Fig. 3.

2.2 Comparison of e^+p to e^-p cross sections

Direct experimental evidence for the contribution of 2γ exchange can be obtained by comparing the ratio of e^+p to e^-p cross sections. The interference of the $\mathcal{M}_0$ and $\mathcal{M}^{\gamma\gamma}$ amplitudes has the opposite sign for electron and positron scattering. Since the finite part of the 2γ contribution is negative over most of the range of ε, one would expect to see an enhancement of the ratio of e^+ to e^- cross sections,

$$R^{e^+e^-} \approx 1 - 2\Delta \,, \tag{10}$$

where Δ is defined in (9).

Although the current data on elastic e^-p and e^+p scattering are sparse, there are some experimental constraints from old data taken at SLAC [11,12], Cornell [13], DESY [14] and Orsay [15]. The data are predominantly at low Q^2 and at forward scattering angles, corresponding to large ε ($\varepsilon \geq 0.7$), where the 2γ exchange contribution is small ($\leq 1\%$). Nevertheless, the overall trend in the data reveals a small enhancement in $R^{e^+e^-}$ at the lower ε values, as illustrated in Fig. 4 (which shows a subset of the data, from the SLAC experiments [11,12]).

The data in Fig. 4 are compared with our theoretical results, calculated for several fixed values of Q^2 ($Q^2 = 1$,

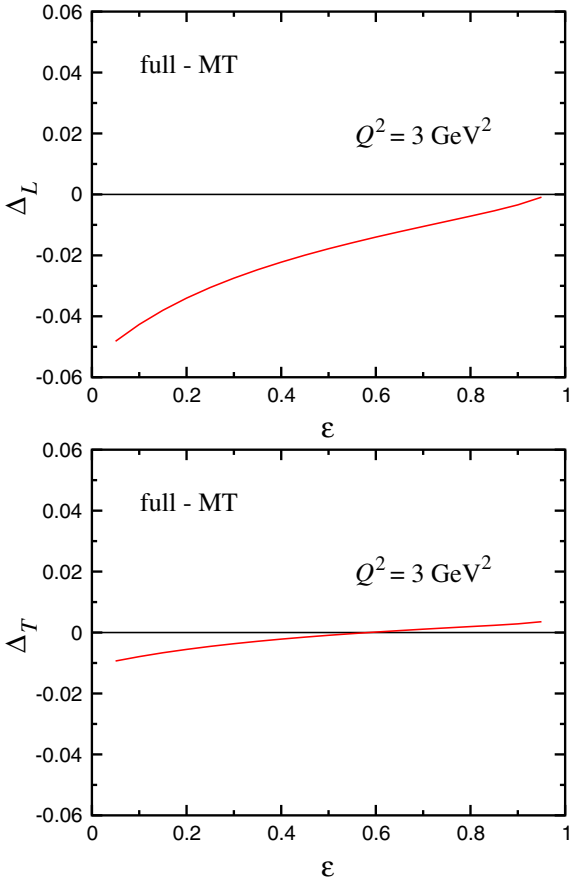

Fig. 5. Ratio of the finite part (with respect to the IR contribution in (8)) of the 2γ correction relative to the Born term, for longitudinal (*top*) and transverse (*bottom*) recoil proton polarization, for $Q^2 = 3$ GeV^2

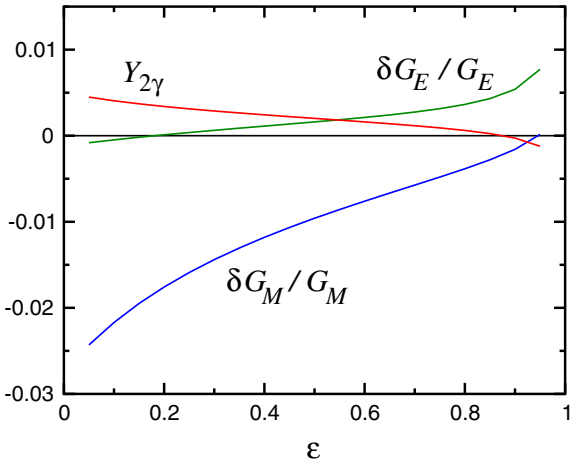

Fig. 6. Finite 2γ contributions (defined with respect to the Mo-Tsai IR result [5]) to the real parts of the G_E, G_M and $Y_{2\gamma}$ form factors of the proton at $Q^2 = 3$ GeV^2

3 and 6 GeV^2). The results are in good agreement with the data, although the errors on the data points are quite large. Clearly better quality data at backward angles, where an enhancement of up to $\sim 10\%$ is predicted, would be needed for a more definitive test of the 2γ exchange mechanism. An experiment [16] using a beam of e^+e^- pairs produced from a secondary photon beam at Jefferson Lab will make simultaneous measurements of e^-p and e^+p elastic cross sections up to $Q^2 \sim 2$ GeV^2. A proposal to perform a precise ($\sim 1\%$) comparison of e^-p and e^+p scattering at $Q^2 = 1.6$ GeV^2 and $\varepsilon \approx 0.4$ has also been made at the VEPP-3 storage ring [17].

3 Polarized electron–proton scattering

The results of the 2γ exchange calculation in the previous section give a clear indication of a sizable correction to the LT-separated data at moderate and large Q^2. We now look at the effect of 2γ exchange on the polarization transfer results. Specifically, we have recalculated $\mathcal{M}^{\gamma\gamma}$ for the case of a polarized incident electron, and a polarized recoil proton.

The 2γ exchange contribution relative to the Born term is shown in Fig. 5 for the cases of longitudinal (Δ_L) and transverse (Δ_T) proton polarization for $Q^2 = 3$ GeV^2. In analogy with the unpolarized case (see (9)), the spin-dependent corrections $\Delta_{L,T}$ are defined as the finite parts of the 2γ contributions relative to the IR expression from Mo & Tsai [5], which are independent of polarization [18].

The corrections for Δ_L show a more dramatic dependence on ε than those for Δ_T. As with the unpolarized case, the effect is generally larger at small ε than at large ε.

While the 2γ corrections clearly play a vital role in resolving most of the form factor discrepancy, it is instructive to understand the origin of the effect on R with respect to contributions to the individual G_E^p and G_M^p form factors. In general the amplitude for elastic scattering of an electron from a proton, beyond the Born approximation, can be described by three (complex) form factors, $\widetilde{F}_1$, $\widetilde{F}_2$ and $\widetilde{F}_3$, in terms of which the electromagnetic current can be written as [19,20]

$$\Gamma^\mu = \widetilde{F}_1\,\gamma^\mu \;+\; \widetilde{F}_2\,\frac{i\sigma^{\mu\nu}q_\nu}{2M} \;+\; \widetilde{F}_3\,\frac{\not{K} P^\mu}{M^2}\;, \qquad (11)$$

where $K^\mu = (p_1^\mu + p_3^\mu)/2$, $P^\mu = (p_2^\mu + p_4^\mu)/2$. The functions $\widetilde{F}_{1,2,3}$ (both real and imaginary parts) are in general functions of Q^2 and ε, or the variable $\nu \equiv K \cdot P$, which is related to ε by $\varepsilon = \big(\nu^2 - M^4\tau(1+\tau)\big) \,/\, \big(\nu^2 + M^4\tau(1+\tau)\big)$. In the 1γ exchange limit the $\widetilde{F}_{1,2}$ functions approach the usual (real) Dirac and Pauli form factors, while the new form factor $\widetilde{F}_3$ exists only at the 2γ level and beyond,

$$\widetilde{F}_{1,2}(Q^2,\nu) \to F_{1,2}(Q^2)\;, \qquad (12)$$

$$\widetilde{F}_3(Q^2,\nu) \to 0\;. \qquad (13)$$

Alternatively, the current can be expressed in terms of the generalized (complex) Sachs electric and magnetic form factors, $\widetilde{G}_M = G_M + \delta G_M$ and $\widetilde{G}_E = G_E + \delta G_E$. The cross section and polarization observables, up to order α^2, can be written in terms of these functions [19,20]. The

form factor $\widetilde{F}_3$ has been expressed in terms of the ratio [19]

$$Y_{2\gamma} = \mathrm{Re}\left(\frac{\nu\widetilde{F}_3}{M^2 G_M}\right) \ . \tag{14}$$

In Fig. 6 we show the contributions of 2γ exchange to the (real parts of the) proton G_E and G_M form factors, and the ratio $Y_{2\gamma}$, evaluated at $Q^2 = 3$ GeV^2.

It is interesting to observe that the 2γ correction to G_M is significantly larger than that to G_E for $\varepsilon \leq 0.8$, and has a significant ε dependence (cf. [21]). The new correction $Y_{2\gamma}$ is smaller than that extracted in the phenomenological analysis [19] under the assumption that the entire form factor discrepancy is due to the new $\widetilde{F}_3$ contribution.

4 Summary

We have presented an overview of the effects of 2γ exchange in elastic electron–proton scattering, taking particular account of the effects of nucleon structure. Consistent with the simple model used in our earlier investigation [8], we find that inclusion of 2γ exchange reduces the G_E^p/G_M^p ratio extracted from LT-separated cross section data, and resolves a significant amount of the discrepancy with the polarization transfer results.

At higher Q^2 we find strong deviations from linearity, especially at small ε, which can be tested in future high-precision cross section measurements. There is some residual model-dependence in the calculation of the 2γ amplitude arising from the choice of form factors at the internal $\gamma^* NN$ vertices in the loop integration. This dependence, while not overwhelming, will place limitations on the reliability of the LT separation technique in extracting high-Q^2 form factors. On the other hand, the size of the 2γ contributions to elastic scattering could be determined from measurement of the ratio of $e^- p$ to $e^+ p$ elastic cross sections, which are uniquely sensitive to 2γ exchange effects.

We have also generalized our analysis to the case where the initial electron and recoil proton are polarized, as in the polarization transfer experiments. While the 2γ corrections can be as large as $\sim 4-5\%$ at small ε for $Q^2 \sim 6$ GeV^2, since the polarization transfer measurements are performed typically at large ε we find the impact on the extracted G_E^p/G_M^p ratio to be quite small, amount to $\leq 3\%$ suppression at the highest Q^2 value.

Contributions from excited states, such as the Δ and heavier, may modify the quantitative analysis presented here. Naively, one could expect their effect to be suppressed because of the larger masses involved. A detailed investigation of the inelastic excitation effects is currently in progress [6].

Acknowledgements. This work was supported in part by NSERC (Canada), DOE grant DE-FG02-93ER-40762, and DOE contract DE-AC05-84ER-40150 under which the Southeastern Universities Research Association operates the Thomas Jefferson National Accelerator Facility.

References

1. R.C. Walker et al.: Phys. Rev. D **49**, 5671 (1994)
2. J. Arrington: Phys. Rev. C **68**, 034325 (2003)
3. J. Arrington: nucl-ex/0312017
4. M.K. Jones et al.: Phys. Rev. Lett. **84**, 1398 (2000); O. Gayou et al.: Phys. Rev. Lett. **88**, 092301 (2002)
5. L.W. Mo, Y.S. Tsai: Rev. Mod. Phys. **41**, 205 (1969); Y. S. Tsai: Phys. Rev. **122**, 1898 (1961)
6. P.G. Blunden, W. Melnitchouk, J. A. Tjon: in preparation
7. L.C. Maximon, J.A. Tjon: Phys. Rev. C **62**, 054320 (2000)
8. P.G. Blunden, W. Melnitchouk, J.A. Tjon: Phys. Rev. Lett. **91**, 142304 (2003)
9. G. Passarino, M.J. Veltman: Nucl. Phys. B **160**, 151 (1979)
10. Jefferson Lab proposal PR-04-020, J. Arrington spokesperson
11. A. Browman, F. Liu, C. Schaerf: Phys. Rev. **139**, B1079 (1965)
12. J. Mar et al.: Phys. Rev. Lett. **21**, 482 (1968)
13. R.L. Anderson et al.: Phys. Rev. Lett. **17**, 407 (1966); Phys. Rev. **166**, 1336 (1968)
14. W. Bartel et al.: Phys. Lett. B **25**, 242 (1967)
15. B. Bouquet et al.: Phys. Lett. B **26**, 178 (1968)
16. W.K. Brooks et al.: *Beyond the Born approximation: A precise comparison of e^+p and e^-p scattering in CLAS*, Jefferson Lab experiment E04-116 (2004)
17. J. Arrington et al.: *Two-photon exchange and elastic scattering of electrons/positrons on the proton*, proposal for an experiment at VEPP-3 (2004), nucl-ex/0408020
18. L.C. Maximom, W.C. Parke: Phys. Rev. D **61**, 045502 (2000)
19. P.A.M. Guichon, M. Vanderhaeghen: Phys. Rev. Lett. **91**, 142303 (2003)
20. Y.C. Chen, A. Afanasev, S.J. Brodsky, C.E. Carlson, M. Vanderhaeghen: Phys. Rev. Lett. **93**, 122301 (2004)
21. J. Arrington: hep-ph/0408261